More absorptive AVF inversion - attenuating incidence media and general dispersion laws

Kris Innanen

ABSTRACT

In this paper we review our 2009 discussion of direct inversion of absorptive reflectivity, discuss further the requirements for practical implementation, and extend the results to attenuating incidence media and more general attenuation laws. It is the case that frequency-dependent seismic field data anomalies, appearing in association with low-Q targets, have, on occasion, been attributed to the presence of a strong absorptive reflection coefficient. This "absorptive reflectivity" represents a potent, and largely untapped, source of information for determining subsurface rock mechanical properties, and may be of particular relevance to, e.g., reservoir characterization. It would most likely be encountered where a predominantly elastic/non-attenuating overburden is suddenly interrupted by a highly attenuative target. Series expansions of absorptive reflection coefficients about small parameter contrasts and incidence angles can expose these anomalies to analysis, either frequency-by-frequency (AVF) or angle-by-angle (AVA). Within this framework, for instance, variations in P-wave velocity and Q may be separately estimated through a range of direct formulas, both linear and with nonlinear corrections. The latter come to the fore when a contrast from an incidence medium $Q \approx \infty$ (i.e., acoustic/elastic) to a target medium $Q \approx 5 - 10$ is encountered, in which case the linearized estimate may be in error by as much as 50%. Algorithmically, it is a differencing of the reflection coefficient across frequencies that separates Q variations from variations in other parameters. This holds for both two-parameter (P-wave velocity and Q) problems and five-parameter anelastic problems, and would appear to be a general feature of direct absorptive inversion.

INTRODUCTION

The geophysics literature contains numerous reports of frequency-dependent seismic data anomalies associated with attenuating targets. Some researchers have attributed these to the presence of a strong absorptive reflection coefficient, which, indeed, according to wave theory, places a characteristic imprint on the data. This represents a potentially important source of information of direct relevance to, e.g., reservoir characterization. The objective of the work presented here is to develop theoretical insight into the problem of extracting this information. We know in advance that, at least for the case of constant density an-acoustic media, the absorptive reflection coefficient (discussed in theory by, e.g., White, 1965; Borcherdt, 1977; Kjartansson, 1979; Krebes, 1984; Lam et al., 2004; de Hoop et al., 2005; Borcherdt, 2009) can be used to determine, within a linear approximation, the parameter changes responsible for the reflection. This was established by reducing the general absorptive inverse scattering problem to the case of inversion for the properties of a single interface (Innanen and Weglein, 2007). Here we examine the single-interface problem in its own right, and in significantly greater detail. We derive a range of formulas for the direct estimation of target absorptive medium properties, both in linearized forms and with nonlinear corrections, given the reflection coefficient associated with a specific primary event as input. Practically, this corresponds to situations in which the primary reflection from a

target of interest can be identified and isolated, and its angle- and frequency-dependence analyzed. Examples of these formulas were presented at both the EAGE and SEG annual meetings in 2010 (Innanen, 2010b,a).

An absorptive reflection coefficient can be analyzed mathematically by considering either its frequency variations (i.e., AVF), or its angle variations (i.e., AVA). Both have been studied. Numerically, absorption-specific reflection coefficient variability has been reported at large angles when synthetic viscoelastic data were examined at fixed frequencies (Samec and Blangy, 1992). And more recently, field data variability associated with low-Q, fluid filled reservoirs has been attributed to "strongly frequency dependent" reflection coefficients (Odebeatu et al., 2006). This latter observation appears to be supported by other recent investigations and discussions (Chapman et al., 2006; Lines et al., 2008; Ren et al., 2009; Quintal et al., 2009).

Therefore, and notwithstanding the variety of mechanisms that could explain a frequency-dependent reflection (Castagna et al., 2003), there appears to be sufficient evidence of absorptive reflectivity to warrant a theoretical study of the inverse problem. We will emphasize in particular the issue of separability — if, and how, it is possible to determine variations in multiple an-acoustic or anelastic medium properties, including Q, occurring simultaneously at a reflecting boundary. The key features of the problem are captured by examining the simple, absorptive reflection coefficient which arises due to contrasts in P-wave velocity and a nearly constant quality factor Q. We express the reflection coefficient in terms of a variety of different plane-wave variables, expand it about small parameter contrasts and incidence angles, and directly invert these series to determine the properties of the target.

The medium of incidence is here assumed to be acoustic/elastic, i.e., with $Q \rightarrow \infty$. This corresponds to problems in which attenuation is low or negligible in the overburden above an absorptive target. The rationale for this choice is not that an elastic or acoustic overburden transitioning to a highly attenuative target medium is the most common configuration of attenuating geological structures. Rather, the rationale is that it is under these circumstances that the absorptive signature of interest is strongest, and therefore most likely to be measurable. Geophysically these conditions could be encountered when characterizing a gas-saturated reservoir target, or a seafloor target. In a later section we show parenthetically that, in the case in which attenuation is present above the target, the inversion equations retain similar forms.

We also consider a set of other reasonable deviations from the two-parameter model, examining each of (1) a general attenuation law (as opposed to the very specific nearly constant Q model we use), (2) the effect of variations in further parameters, and (3) some examples of and issues surrounding an extension of these results to the anelastic case. The aim will be to distinguish the general insights brought by the two-parameter problem from algorithmic niceties necessary for any specific (and likely more sophisticated) implementations of these inverse ideas.

The inversion methodology we will use is, in essence, a simplified form of inverse scattering. It represents a modification of a framework that has led elsewhere to direct

acoustic and elastic target identification (Zhang and Weglein, 2009a,b). In addition to the added complication of absorbing media, in our approach rather than posing the full inverse scattering problem, thereafter reducing to the case of a single interface, we begin with a representation of the wave response of a single interface, i.e., the reflection coefficient. The cost is a loss of generality and applicability to problems outside of the AVF/AVA framework of interest in this paper, but we benefit in that the formulas are derived rapidly.

ABSORPTIVE WAVE EQUATIONS

Consider a wavefield P_0, propagating in a two-dimensional, homogeneous, source-free, non-absorptive medium (medium 0, the medium of incidence) according to

$$\left[\nabla^2 + \frac{\omega^2}{c_0^2}\right] P_0(x, z, \omega) = 0, \tag{1}$$

and consider P_1 propagating in an absorptive medium (medium 1, the target medium) according to

$$\left[\nabla^2 + \frac{\omega^2}{c^2}\left(1 + \frac{F(\omega)}{Q}\right)^2\right] P_1(x, z, \omega) = 0, \tag{2}$$

where

$$F(\omega) = \frac{i}{2} - \frac{1}{\pi}\log\left(\frac{\omega}{\omega_r}\right), \tag{3}$$

and ω_r is a reference frequency. Equation (2) is consistent with the nearly-constant Q model reviewed by Aki and Richards (2002). Physically, these equations describe acoustic and an-acoustic waves propagating through media of constant density. Fourier transforming equations (1)–(2) with respect to x and z, we have

$$k_x^2 + k_z^2 = \frac{\omega^2}{c_0^2}, \tag{4}$$

and

$$k_x^2 + k_z'^2 = \frac{\omega^2}{c^2}\left(1 + \frac{F(\omega)}{Q}\right)^2, \tag{5}$$

the first of which implies a range of possible relationships based on plane wave geometry, e.g.:

$$\begin{aligned} k_x &= \frac{\omega}{c_0}\sin\theta, \\ k_z &= \frac{\omega}{c_0}\cos\theta, \end{aligned} \tag{6}$$

where θ represents the plane wave angle measured away from the direction of positive z, and k_x and k_z are the Fourier conjugates of x and z respectively.

ABSORPTIVE REFLECTION COEFFICIENTS

If a plane wave P_0 is incident upon a planar boundary, oriented perpendicularly to z and separating medium 0 from medium 1, continuity of the field (e.g., pressure) and its derivative across the interface requires that there be a reflection coefficient

$$R = \frac{k_z - k_z'}{k_z + k_z'}, \tag{7}$$

which, because of equations (3)–(5), we anticipate to be complex, frequency-dependent, and expressive of the an-acoustic properties of the target medium in some hopefully useful ways.

We will examine R at both normal and oblique incidence. In the latter case there is some room for choice in studying its behavior. For instance, if frequency ω is held fixed as a parameter, we have one kind of angular behavior:

$$R(\omega,\theta) = \frac{c\cos\theta - c_0\left[1+Q^{-1}F(\omega)\right]\sqrt{1-\frac{c^2}{c_0^2}\left[1+Q^{-1}F(\omega)\right]^{-2}\sin^2\theta}}{c\cos\theta + c_0\left[1+Q^{-1}F(\omega)\right]\sqrt{1-\frac{c^2}{c_0^2}\left[1+Q^{-1}F(\omega)\right]^{-2}\sin^2\theta}}, \tag{8}$$

whereas, if k_z is a parameter, the θ behavior is modified:

$$R(k_z,\theta) = \frac{c\cos\theta - c_0\left[1+Q^{-1}F_{kz}(\theta)\right]\sqrt{1-\frac{c^2}{c_0^2}\left[1+Q^{-1}F_{kz}(\theta)\right]^{-2}\sin^2\theta}}{c\cos\theta + c_0\left[1+Q^{-1}F_{kz}(\theta)\right]\sqrt{1-\frac{c^2}{c_0^2}\left[1+Q^{-1}F_{kz}(\theta)\right]^{-2}\sin^2\theta}}, \tag{9}$$

where

$$F_{kz}(\theta) = \frac{i}{2} - \frac{1}{\pi}\log\left(\frac{k_z c_0}{\omega_r\cos\theta}\right). \tag{10}$$

We will not use it in this paper, but furthermore if k_x is a parameter, we again discern a slightly altered θ variability in R:

$$R(k_x,\theta) = \frac{c\cos\theta - c_0\left[1+Q^{-1}F_{kx}(\theta)\right]\sqrt{1-\frac{c^2}{c_0^2}\left[1+Q^{-1}F_{kx}(\theta)\right]^{-2}\sin^2\theta}}{c\cos\theta + c_0\left[1+Q^{-1}F_{kx}(\theta)\right]\sqrt{1-\frac{c^2}{c_0^2}\left[1+Q^{-1}F_{kx}(\theta)\right]^{-2}\sin^2\theta}}, \tag{11}$$

where

$$F_{kx}(\theta) = \frac{i}{2} - \frac{1}{\pi}\log\left(\frac{k_x c_0}{\omega_r\sin\theta}\right). \tag{12}$$

The special case $\theta = 0$ in equation (8) corresponds to R at normal incidence.

The variation of R with ω, θ, etc. above provides the information by which parameters of interest will ultimately be determined. For this determination to be possible, every realizable set of target medium properties must generate a unique $R(\omega,\theta)$. Both qualitative

evidence that this is the case, and a sense of how the variations in the reflection coefficient might be used to determine target properties c and Q, may be derived from an examination of plots of R. In Figure 1 we focus on the frequency dependence of R by setting $\theta = 0$, and plotting $R(\omega)$ for a range of target Q values, with P-wave velocities fixed at $c_0 = 1500$m/s and $c = 1600$m/s. In the top left panel we observe that, especially at low values of Q (5-100), the frequency-dependence of the real part of R exhibits clear variability with target Q value. This is an early indication that relative differences in R from frequency to frequency might serve to distinguish one target Q value from another. In contrast, in the top right panel, we see that the distinction (at normal incidence) between one target P-wave velocity and another must apparently derive from the absolute magnitudes of the real part of R. In both cases the imaginary part of R (bottom panels) would appear to carry much less useful information.

In Figure 2 the same variability is viewed in the form of θ variations with a fixed depth wavenumber k_z, using equation (9). The top row involves a k_z at one-fifth of its maximum value (i.e., $k_z = 0.1$ for k_z normalized such that $\max(k_z) = 0.5$), and the bottom row involves a k_z at one-half of its maximum value (i.e., $k_z = 0.25$ for k_z normalized such that $\max(k_z) = 0.5$). In the top left and bottom left panels, $R(k_z, \theta)$ is plotted for a range of target Q values. We again observe that the variation of R with θ changes as target Q changes, in particular at low values, and so we have the general expectation that relative AVA variations may be adequate, as the AVF variations were, as means to determine a target Q. In the right panels, $R(k_z, \theta)$ is plotted for a range of target P-wave velocity values. The expected AVA signature of the P-wave velocity contrast is visible.

SERIES EXPANSIONS AND APPROXIMATIONS OF R

We consider three quantities embedded in R that are, from a geophysical point of view, sometimes small, but not always. They are (1) angle of incidence, (2) the relative change in P-wave velocity (from c_0 to c), and (3) the relative change in the inverse quality factor (from 0 to Q^{-1}). As measures of the latter two we define

$$\begin{aligned} a_c &= 1 - \frac{c_0^2}{c^2}, \\ a_Q &= \frac{1}{Q}, \end{aligned} \tag{13}$$

and as a measure of the first, we consider R as a function of $\sin^2\theta$. The inversion scheme used in the coming sections relies on series expansions of the reflection coefficients in equations (8)–(9), in orders of these quantities.

In equations (8)–(11), we observe that, depending on the parametrization, the presence of dispersion can bring an additional level of complexity in the θ dependence beyond the

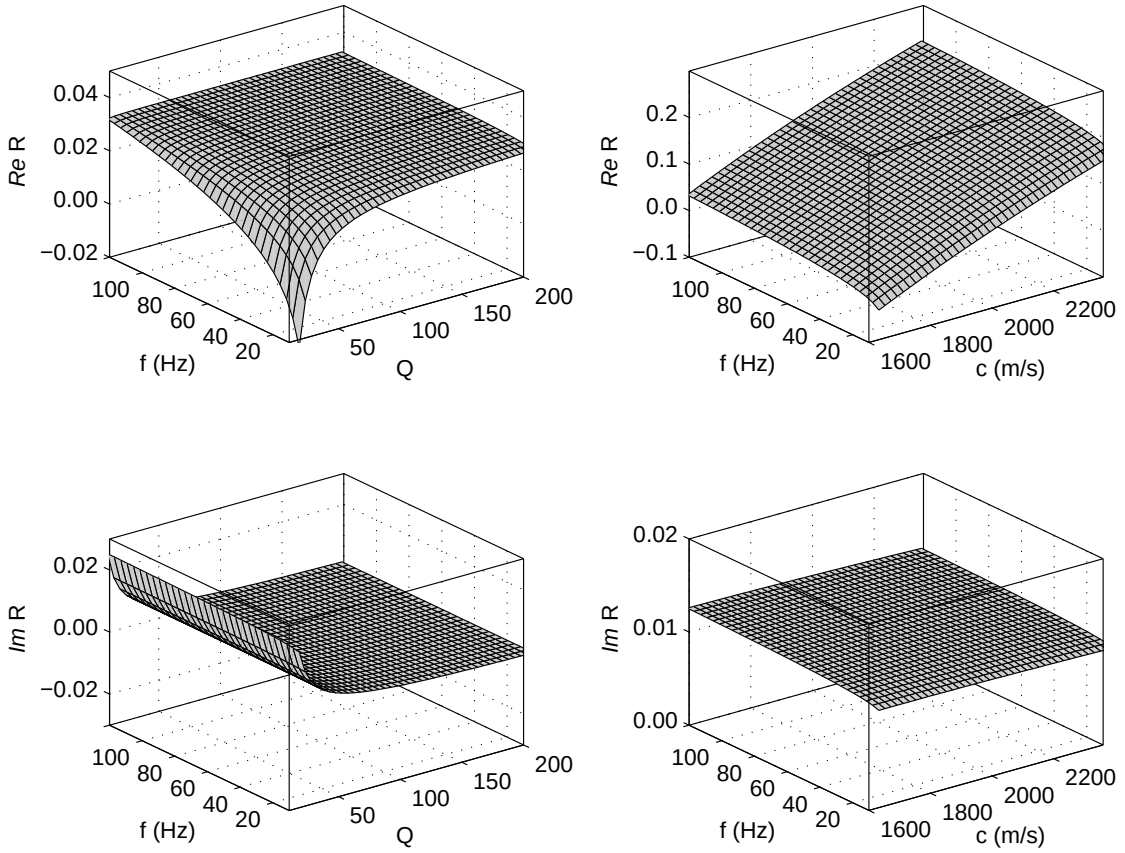

FIG. 1. Absorptive reflection coefficient R at normal incidence, as expressed in equation (8) with $\theta = 0$, with c_0 =1500m/s. Left column: R for a range of frequency and Q values (c fixed at 1600m/s). Right column: R for a range of frequency and c values (Q fixed at 10). Each fixed Q value produces, in the real part of R, a unique associated signature in the frequency domain (top left).

constant-density acoustic case. If ω is fixed as a parameter, it does not, and R expands as

$$\begin{aligned} R(\omega,\theta) = &\left[\left(\frac{1}{4}a_c - \frac{1}{2}F(\omega)a_Q\right) + \left(\frac{1}{8}a_c^2 + \frac{1}{4}F^2(\omega)a_Q^2\right) + ...\right]\left(\sin^2\theta\right)^0 \\ &+ \left[\left(\frac{1}{4}a_c - \frac{1}{2}F(\omega)a_Q\right) + \left(\frac{1}{4}a_c^2 - \frac{1}{2}F(\omega)a_c a_Q + \frac{3}{4}F^2(\omega)a_Q^2\right) + ...\right]\left(\sin^2\theta\right)^1 \\ &+ \left[\left(\frac{1}{4}a_c - \frac{1}{2}F(\omega)a_Q\right) + \left(\frac{3}{8}a_c^2 - F(\omega)a_c a_Q + \frac{5}{4}F^2(\omega)a_Q^2\right) + ...\right]\left(\sin^2\theta\right)^2 \\ &+ ... \ . \end{aligned} \tag{14}$$

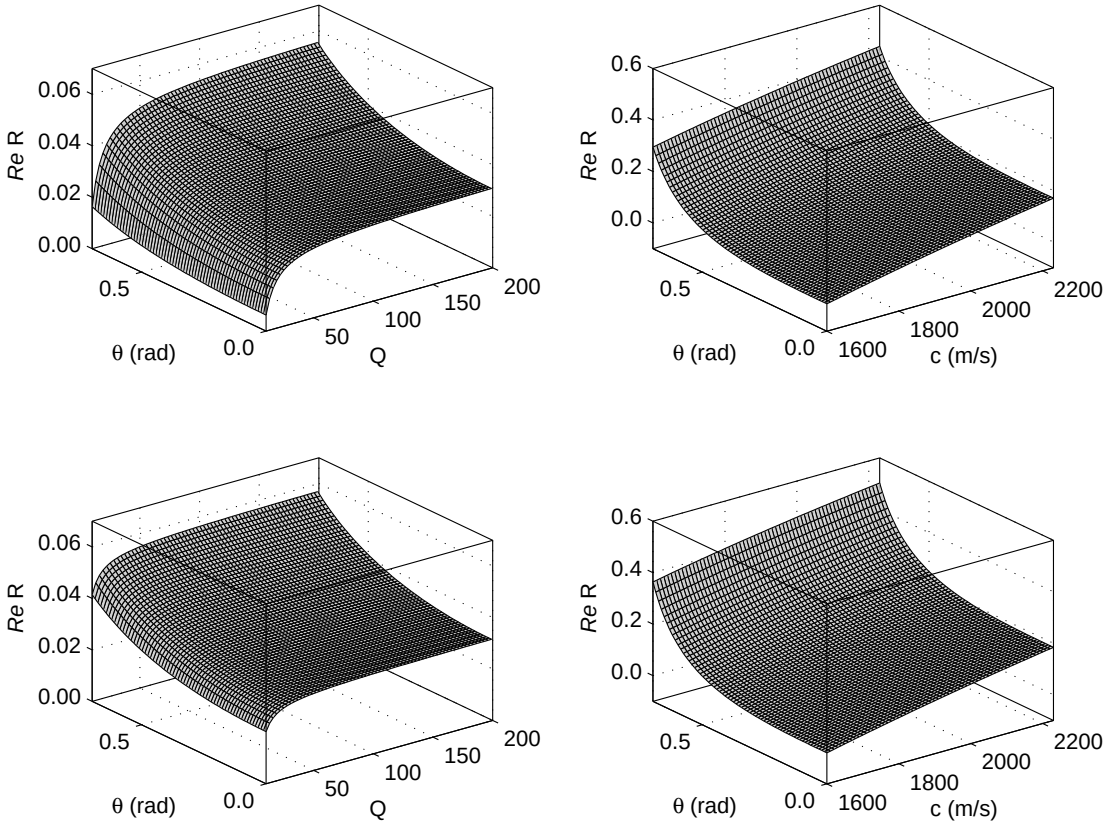

FIG. 2. Absorptive reflection coefficient $R_{kz}(\theta)$, as expressed in equation (9), with c_0 =1500m/s, plotted for a range of target Q values with fixed $c = 1600$m/s (left column), and c values with fixed $Q = 10$ (right column) for two values of k_z. Top row: fixed normalized $k_z = 0.1$; bottom row: fixed normalized $k_z = 0.25$ (in both cases $k_{zmax} = 0.5$).

If k_z is a parameter, however, the coefficients of the $\sin^2\theta$ expansion of R take on a uniquely dispersive character:

$$\begin{aligned}\tilde{R}(k_z,\theta) = &\left\{\left[\frac{1}{4}a_c - \frac{1}{2}\tilde{F}_{kz}a_Q\right] + \left[\frac{1}{8}a_c^2 + \frac{1}{4}\tilde{F}_{kz}^2 a_Q^2\right] + ...\right\}\left(\sin^2\theta\right)^0 \\ &+ \left\{\left[\frac{1}{4}a_c - \left(\frac{1}{2}\tilde{F}_{kz} - \frac{1}{4\pi}\right)a_Q\right] + \left[\frac{1}{4}a_c^2 - \frac{1}{2}\tilde{F}_{kz}a_c a_Q + ...\right] + ...\right\}\left(\sin^2\theta\right)^1 \\ &+ \left\{\left[\frac{1}{4}a_c - \left(\frac{1}{2}\tilde{F}_{kz} - \frac{3}{8\pi}\right)a_Q\right] + \left[\frac{3}{8}a_c^2 - \left(\tilde{F}_{kz} - \frac{1}{4\pi}\right)a_c a_Q\right.\right. \\ &\left.\left. + \left(\frac{5}{4}\tilde{F}_{kz}^2 - \frac{7}{8\pi}\tilde{F}_{kz} + \frac{1}{16\pi^2}\right)a_Q^2\right] + ...\right\}\left(\sin^2\theta\right)^2 + ...,\end{aligned} \tag{15}$$

where

$$\tilde{F}_{kz} = \frac{i}{2} - \frac{1}{\pi}\log\left(\frac{k_z c_0}{\omega_r}\right). \tag{16}$$

Alternatively, if $R(k_z, \theta)$ is expanded only in the angle variations that occur absent dispersion, we have instead the useful form

$$\begin{aligned} R(k_z,\theta) = & \left[\left(\frac{1}{4}a_c - \frac{1}{2}F_{kz}(\theta)a_Q\right) + \left(\frac{1}{8}a_c^2 + \frac{1}{4}F_{kz}^2(\theta)a_Q^2\right) + ...\right]\left(\sin^2\theta\right)^0 \\ & + \left[\left(\frac{1}{4}a_c - \frac{1}{2}F_{kz}(\theta)a_Q\right) + \left(\frac{1}{4}a_c^2 - \frac{1}{2}F_{kz}(\theta)a_c a_Q + \frac{3}{4}F_{kz}^2(\theta)a_Q^2\right) + ...\right]\left(\sin^2\theta\right)^1 \\ & + \left[\left(\frac{1}{4}a_c - \frac{1}{2}F_{kz}(\theta)a_Q\right) + \left(\frac{3}{8}a_c^2 - F_{kz}(\theta)a_c a_Q + \frac{5}{4}F_{kz}^2(\theta)a_Q^2\right) + ...\right]\left(\sin^2\theta\right)^2 \\ & + ... \ . \end{aligned} \tag{17}$$

Equations (14) and (17) will be used to pose the main inverse AVF and AVA problems; in a later section we will alter these expansions to incorporate, alternatively, generalized attenuation laws, as well as density variations and anelastic phenomena. These are forward modeling expressions: given incidence and target medium properties, we form a_c and a_Q using equation (13), and substitute them into the above formulas for R. Truncating any of these series expansions at first or second order in the parameter perturbations, we obtain simple and straightforward approximations of the reflection coefficients. For instance, retaining terms in equation (17) that are linear in the parameter perturbations and in $\sin^2\theta$ results in the approximation

$$R(k_z,\theta) \approx \left[\left(\frac{1}{4}a_c - \frac{1}{2}F_{kz}(\theta)a_Q\right)\right]\left(1+\sin^2\theta\right). \tag{18}$$

In Figure 3 the accuracy of first and second order approximations to $R(k_z, \theta)$ is illustrated; as one would expect, at large parameter perturbations and large angles, the approximation error of the first order approximation grows. This is technically true of the second order approximation also, but the error is reduced and does not grow significantly until comparatively large angles are considered. Based in particular on the differences in accuracy observable in transitioning from the middle row of Figure 3 (the linear approximation) to the bottom row (truncation after second order), we might reasonably anticipate that second-order effects will non-negligibly influence absorptive inversion for targets with $Q < 50$, which is the Q range of interest in this paper. Hence, we will define as part of our inverse objective the proper incorporation of the nonlinearity of the data-parameter relationship.

ABSORPTIVE AVF/AVA INVERSION

The forward problem we consider in this paper is the calculation of R over a range of the variables k_x and ω (i.e., the Fourier conjugates of offset and time respectively, which may subsequently be transformed to k_z, θ as desired), given a_c and a_Q. The inverse problem is the exact or approximate determination of a_c and a_Q from values of R over a range of one or more of these variables. The inversion is referred to as AVA or AVF, to correspond to the respective use of angle or frequency as this variable. Any time in the following examples there are two parameters to be solved for, at least two data will be required, and they will be produced by varying the values of either frequency or angle and assuming that R is available at these values. In any practical implementation of these formulas we would

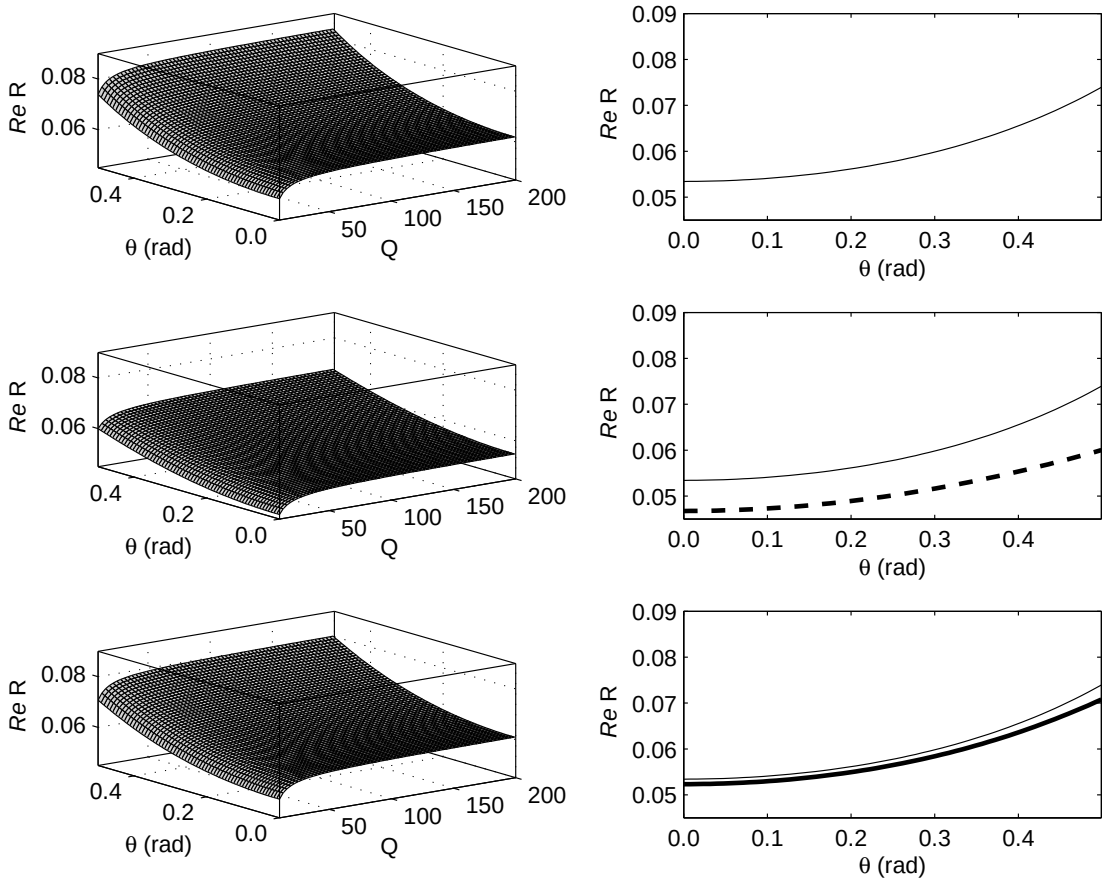

FIG. 3. Absorptive reflection coefficient R, in exact and approximate forms (using equation (9) and truncated versions of equation (17) respectively), plotted over a range of oblique incidence angles and target Q values, with c_0 =1500m/s and c =1700m/s and fixed normalized $k_z = 0.3$. Left column, from top to bottom: surface plots of exact, linear, and nonlinear (second order) approximations. Right column: extractions from left column, for fixed target $Q = 10$, in which the exact R is represented with a solid line, the linear R with a dashed line, and the nonlinear (second order) R with a bold solid line.

naturally use as many data as we had, and fit the parameters with an appropriate regression. Here, since the objective is to gain theoretical insight into the inverse problem, we will assume exact data, in which case, since there are at most two parameters to solve for, we will use at most two data. If the number of parameters becomes larger, say N, a minimum of N data are of course required.

AVF inversion at normal incidence

We will begin to treat the AVF inverse problem by considering a wave field impinging at normal incidence on a plane contrast in c and Q. Setting $\theta = 0$ in equation (14), the requisite R has the form

$$R(\omega) = \left(\frac{1}{4}a_c - \frac{1}{2}F(\omega)a_Q\right) + \left(\frac{1}{8}a_c^2 + \frac{1}{4}F^2(\omega)a_Q^2\right) + ... \quad . \tag{19}$$

This expression is inverted by forming inverse series $a_c = a_{c_1} + a_{c_2} + ...$, and $a_Q = a_{Q_1} + a_{Q_2} + ...$, substituting them into equation (19), equating like orders, and summing the sequentially-determined components of a_c and a_Q. Using R at two angular frequencies, ω_1 and ω_2, we obtain, at first order,

$$\begin{aligned} a_{Q_1}(\omega_1, \omega_2) &= -2 \left[\frac{R(\omega_1) - R(\omega_2)}{F(\omega_1) - F(\omega_2)} \right] \\ a_{c_1}(\omega_1, \omega_2) &= -4 \left[\frac{F(\omega_2)R(\omega_1) - F(\omega_1)R(\omega_2)}{F(\omega_1) - F(\omega_2)} \right], \end{aligned} \tag{20}$$

and at second order

$$\begin{aligned} a_{Q_2}(\omega_1, \omega_2) &= \Delta_{Q_1} a_{Q_1} + \Delta_{Q_2} a_{c_1} \\ a_{c_2}(\omega_1, \omega_2) &= \Delta_{c_1} a_{Q_1} + \Delta_{c_2} a_{c_1}, \end{aligned} \tag{21}$$

where

$$\begin{aligned} \Delta_{Q_1} &= \tfrac{1}{2}[F(\omega_1) + F(\omega_2)], \quad \Delta_{Q_2} = 0, \\ \Delta_{c_1} &= F(\omega_1)F(\omega_2), \qquad\quad \Delta_{c_2} = -\tfrac{1}{2}, \end{aligned} \tag{22}$$

etc. Because of the relatively simple forms, we may also substitute the explicit forms for a_{Q_1} etc. in equations (20) into the nonlinear corrections in equations (21) to see what these solution series look like explicitly in terms of the data (we will not do this for the remainder of the paper):

$$a_Q(\omega_1, \omega_2) = -2 \left[\frac{R(\omega_1) - R(\omega_2)}{F(\omega_1) - F(\omega_2)} \right] + 2[F(\omega_1) + F(\omega_2)] \left[\frac{R(\omega_1) - R(\omega_2)}{F(\omega_1) - F(\omega_2)} \right]^2 + ..., \tag{23}$$

and

$$\begin{aligned} a_c(\omega_1, \omega_2) = &- 4\frac{F(\omega_2)R(\omega_1) - F(\omega_1)R(\omega_2)}{F(\omega_1) - F(\omega_2)} + 4\frac{F(\omega_1)F(\omega_2)[R(\omega_1) + R(\omega_2)]^2}{[F(\omega_1) - F(\omega_2)]^2} \\ &- 8\frac{R^2(\omega_2)F^2(\omega_1) + R^2(\omega_1)F^2(\omega_2)}{[F(\omega_1) - F(\omega_2)]^2} + ... \quad . \end{aligned} \tag{24}$$

Truncating these expressions at first order produces the (absorptive) inverse Born approximation. We note that equations (20)–(24) use the contrast in dispersive properties at the target to drive the inversion: evidently, only if the reflection coefficient varies with frequency, does $a_Q \neq 0$.

In Figure 4 we illustrate the use of these formulas to invert for target c and Q, using as input synthetically derived, exact, R values at normal incidence for an acoustic medium (c_0 =1500m/s) overlying an absorptive medium (with input c =1800m/s, Q =10). Target medium properties are determined using R values at pairs of frequencies $f_1 = \omega_1/2\pi$ and $f_2 = \omega_2/2\pi$ ranging from 2-120 Hz. In the top left panel, the target Q value is recovered to first order for each frequency pair; in the bottom left, to second order. In the top right panel, the target P-wave velocity value is recovered to first order; in the bottom right, to second

order. In addition to the significant increase in accuracy from first to second order, we note that the spurious variation of the linear Q inversion result with experimental variables (in this case frequency), a characteristic of the inverse Born approximation, diminishes as order increases. However, the second-order recovery of the P-wave velocity becomes unstable near the diagonal corresponding to equal frequencies $f_1 = f_2$: proximal frequencies ($f_1 \approx f_2$) evidently affect the conditioning of the second order recovery of c. The explanation for this is evident in equations (23)–(24). None of these formulas should be expected to operate correctly at $f_1 = f_2$, but, in the case of the Q perturbation a_Q, at second-order both the numerator and the denominator approach zero together as $f_1 \to f_2$, which has a stabilizing effect on the nearly-singular cases, whereas in the case of the P-wave velocity perturbation a_c only the denominator does. This behavior reflects the tendency in direct absorptive inversion for velocity to be determined through absolute values of the reflection strengths, and the quality factor through differences in R across frequencies.

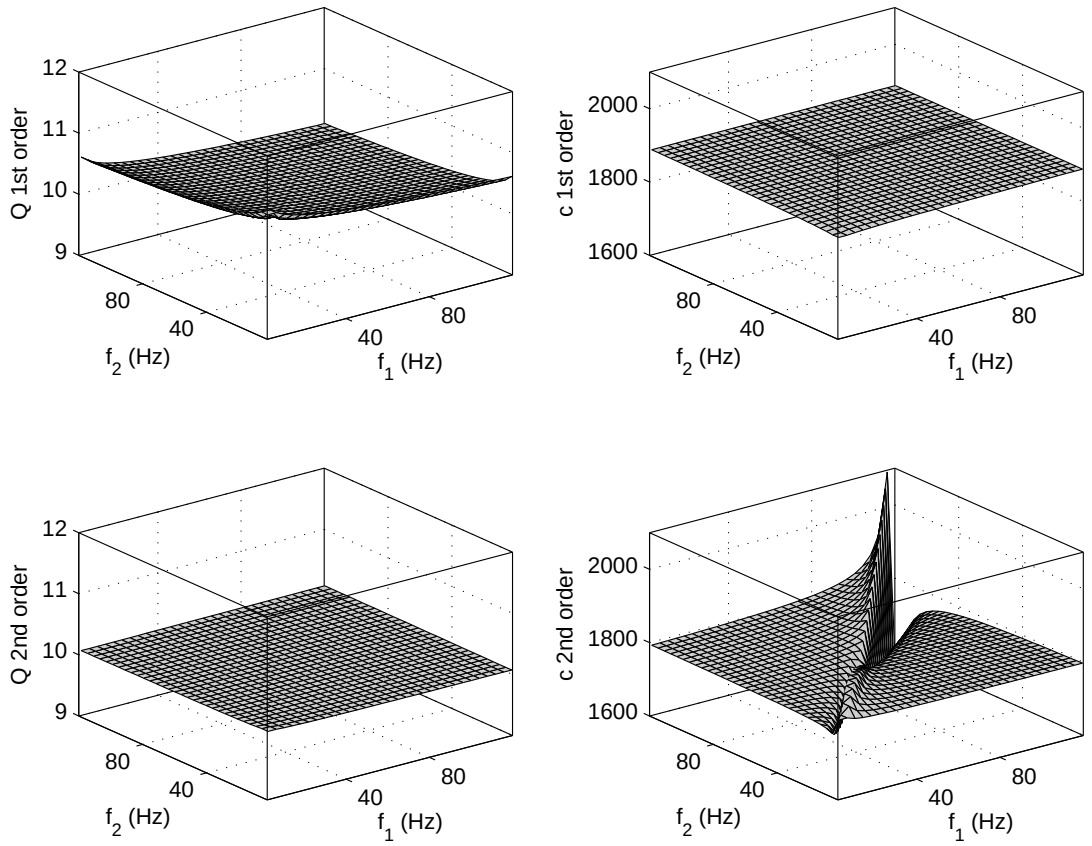

FIG. 4. Target medium properties recovered over a range of frequency pairs, using exact synthetic R values, generated using equation (8) with $\theta = 0$, as input for the AVF inverse formulas in equations (23)–(24). Exact model values are $Q = 10$, $c = 1800$m/s. All c/Q values in rank deficient cases (i.e., where $f_1 = f_2$) are interpolated over.

AVF inversion at oblique incidence

The normal incidence formulas in equations (23)–(24) generalize to oblique incidence straightforwardly. This may be demonstrated within the linear regime for simplicity. Truncating equation (14) at first order in a_c, a_Q, and $\sin^2\theta$, we have

$$R(\omega,\theta) \approx \left(\frac{1}{4}a_c - \frac{1}{2}F(\omega)a_Q\right)\left(1+\sin^2\theta\right), \tag{25}$$

which within this regime of approximation we may re-write as

$$R(\omega,\theta)\cos^2\theta \approx \frac{1}{4}a_c - \frac{1}{2}F(\omega)a_Q. \tag{26}$$

Hence, after correcting the reflection coefficient with an angle-dependent factor $\cos^2\theta$, we recover essentially the same relationship leading to the linear inversion formulas in equation (20). Fixing θ at a desired value θ_0 available within the data, and again using R at two frequencies ω_1 and ω_2, we obtain

$$\begin{aligned} a_Q(\omega_1,\omega_2,\theta_0) &\approx -2\left[\frac{R(\omega_1,\theta_0)\cos^2\theta_0 - R(\omega_2,\theta_0)\cos^2\theta_0}{F(\omega_1)-F(\omega_2)}\right] \\ a_c(\omega_1,\omega_2,\theta_0) &\approx -4\left[\frac{F(\omega_2)R(\omega_1,\theta_0)\cos^2\theta_0 - F(\omega_1)R(\omega_2,\theta_0)\cos^2\theta_0}{F(\omega_1)-F(\omega_2)}\right]. \end{aligned} \tag{27}$$

The second-order terms will have some differences at oblique incidence, but the procedure for determining them is unchanged.

AVA inversion

Variations in a_c and a_Q may also be determined by examining the angle dependence of the reflection coefficient, although this simply makes implicit rather than explicit use of the same frequency dependence. We begin with the expansion of R in equation (17). Again forming inverse series for a_c and a_Q, substituting, and equating like orders, we obtain the formulas

$$\begin{aligned} a_c &= a_{c_1} + a_{c_2} + ..., \\ a_Q &= a_{Q_1} + a_{Q_2} + ..., \end{aligned} \tag{28}$$

in which

$$\begin{aligned} a_{Q_1}(\theta_1,\theta_2) &= -\frac{2}{F_{kz}(\theta_1)-F_{kz}(\theta_2)}\left[\frac{R(k_z,\theta_1)}{1+\sin^2\theta_1} - \frac{R(k_z,\theta_2)}{1+\sin^2\theta_2}\right], \\ a_{c_1}(\theta_1,\theta_2) &= -\frac{4}{F_{kz}(\theta_1)-F_{kz}(\theta_2)}\left[\frac{R(k_z,\theta_1)F_{kz}(\theta_2)}{1+\sin^2\theta_1} - \frac{R(k_z,\theta_2)F_{kz}(\theta_1)}{1+\sin^2\theta_2}\right], \end{aligned} \tag{29}$$

and

$$\begin{aligned} a_{Q_2}(\theta_1,\theta_2) &= \Delta_{Q_1}\, a_{c_1}^2 + \Delta_{Q_2}\, a_{c_1}a_{Q_1} + \Delta_{Q_3}\, a_{Q_1}^2, \\ a_{c_2}(\theta_1,\theta_2) &= \Delta_{c_1}\, a_{c_1}^2 + \Delta_{c_2}\, a_{c_1}a_{Q_1} + \Delta_{c_3}\, a_{Q_1}^2, \end{aligned} \tag{30}$$

etc., where

$$\begin{aligned}
\Delta_{Q_1}(\theta_1,\theta_2) &= \frac{1}{4}\frac{1}{F_{kz}(\theta_1)-F_{kz}(\theta_2)}(\tan^2\theta_1-\tan^2\theta_2)\\
\Delta_{Q_2}(\theta_1,\theta_2) &= \frac{1}{F_{kz}(\theta_1)-F_{kz}(\theta_2)}[F_{kz}(\theta_2)\tan^2\theta_2-F_{kz}(\theta_1)\tan^2\theta_1]\\
\Delta_{Q_3}(\theta_1,\theta_2) &= \frac{1}{2}\frac{1}{F_{kz}(\theta_1)-F_{kz}(\theta_2)}[F_{kz}^2(\theta_1)(1+2\tan^2\theta_1)-F_{kz}^2(\theta_2)(1+2\tan^2\theta_2)]
\end{aligned} \tag{31}$$

and

$$\begin{aligned}
\Delta_{c_1}(\theta_1,\theta_2) &= \frac{1}{2}\frac{1}{F_{kz}(\theta_1)-F_{kz}(\theta_2)}[F_{kz}(\theta_2)(1+\tan^2\theta_1)-F_{kz}(\theta_1)(1+\tan^2\theta_2)]\\
\Delta_{c_2}(\theta_1,\theta_2) &= \frac{1}{F_{kz}(\theta_1)-F_{kz}(\theta_2)}[F_{kz}^2(\theta_1)F_{kz}(\theta_2)(1+2\tan^2\theta_1)-2F_{kz}(\theta_1)F_{kz}^2(\theta_2)(1+2\tan^2\theta_2)]\\
\Delta_{c_3}(\theta_1,\theta_2) &= \frac{2}{F_{kz}(\theta_1)-F_{kz}(\theta_2)}F_{kz}(\theta_1)F_{kz}(\theta_2)(\tan^2\theta_2-\tan^2\theta_1).
\end{aligned} \tag{32}$$

Figure 5 illustrates these formulas in use with synthetically derived, exact, reflection coefficient values as input. The left column illustrates the linear target Q value recovered over a range of angle pairs (top) and the nonlinear correction (bottom). The right column is the corresponding recovered P-wave velocity (actual value 1800m/s). The actual target Q value is 5. In general, the increase in accuracy from the first-order inversion result (top row) to the result including the second-order correction (bottom row) serves to emphasize the importance of incorporating the nonlinearity of the data-parameter relationship, in the presence of low Q values. In this case the linear estimate is in error by roughly 50%.

We also observe a greater variability in accuracy across the range of angle pairs than was evident in the AVF results of the previous section (indeed it is not difficult to devise pathological examples using this particular formulas which exhibit much more marked instability). This is likely a reflection of the more difficult separation problem the AVA approach poses. We are, in essence, forcing the frequency variations due to Q to express themselves in the angle domain, in which there already exists the significant AVA signature of a P-wave velocity contrast. The inverse problem is then obliged to undo this more complicated mixture.

DEVIATIONS FROM THE TWO-PARAMETER VELOCITY/Q MODEL

All inversion procedures, regardless of how complete, face the same problem, namely that in a given situation the wrong parameters are likely being solved for: acoustic parameters as opposed to elastic; isotropic elastic parameters as opposed to anisotropic; etc. In this paper we err on the side of simplicity, the aim being to set out the basic properties of a perturbation-based, single-interface absorptive AVA/AVF modeling and inversion scheme, and, to be sure, the Earth will rarely behave exactly as modeled by equations (1)–(2). As a partial remedy for this, we will treat a representative set of deviations of the Earth away

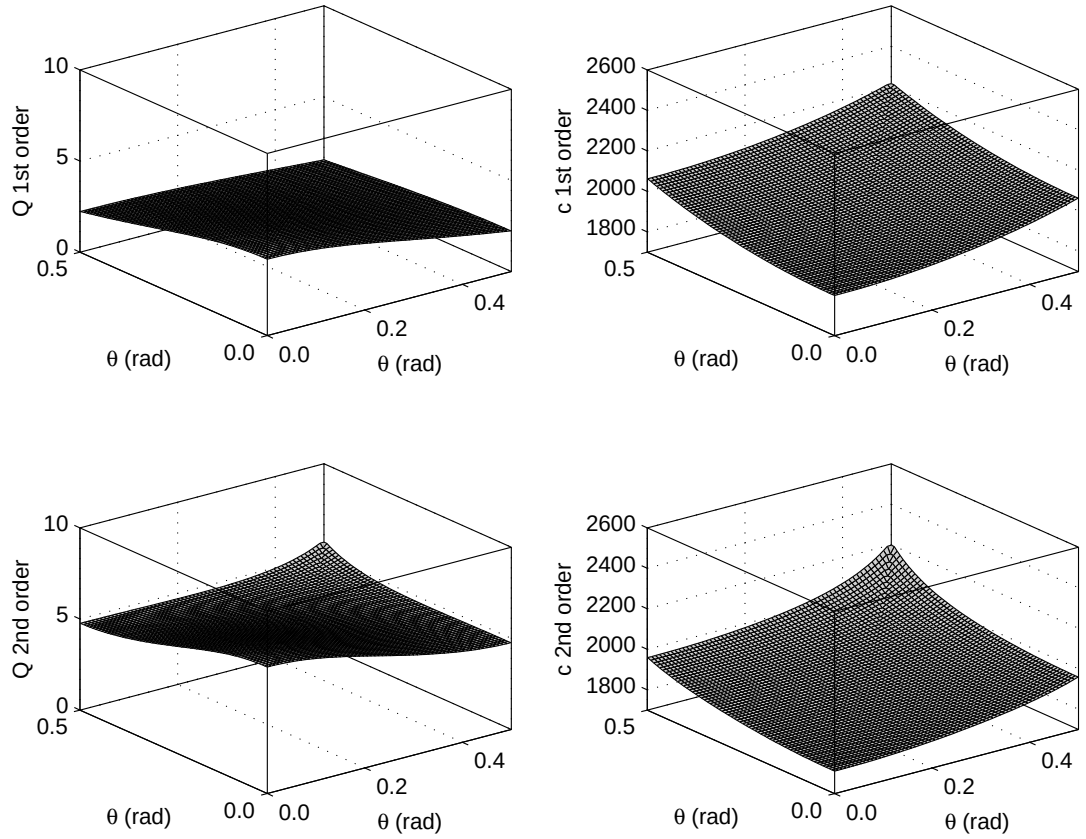

FIG. 5. Target medium properties recovered over a range of angle pairs, using exact synthetic R values, generated using equation (9), as input for the AVA inverse formulas in equations (28)–(30). Exact model values are $Q = 5$, $c_0 = 1500$m/s and $c = 1800$m/s, with fixed normalized $k_z = 0.25$, roughly at the midpoint of the available wavenumber range. All c/Q values in rank deficient cases (i.e., where $\theta_1 = \theta_2$) are interpolated over. First order (inverse Born) estimation of target c and Q values (top) are compared against second order corrected values.

from the two-parameter model we have thus far considered. The point will be to provide a sense of what is general about the formulas in the previous section versus what is special, thereby pointing an interested researcher towards ways to adapt the basic ideas we are espousing to fit with a variant absorptive problem that may be at hand.

General attenuation law

First we consider the possibility that a more general absorption law than that in equation (2) is required to adequately explain data variations. The problem remains tractable, but barely so. To see this, let us begin as we have before, with the reflection coefficient associated with a plane contrast in absorptive medium properties, but this time assume that the propagation constant in the target medium, rather than $K = \omega c^{-1}(1 + FQ^{-1})$, is

$$K = \frac{\omega}{c} + i\nu(\omega) + \mathcal{H}[\nu(\omega)], \tag{33}$$

where ν is a general frequency dependent attenuation coefficient and $\mathcal{H}[\cdot]$ is the Hilbert transform (Aki and Richards, 2002). At normal incidence, the general attenuation case leads to a reflection coefficient of the form

$$R(\omega) = \frac{1 - \frac{c_0}{c} - \omega^{-1} c_0 \left\{ i\nu(\omega) + \mathcal{H}[\nu(\omega)] \right\}}{1 + \frac{c_0}{c} + \omega^{-1} c_0 \left\{ i\nu(\omega) + \mathcal{H}[\nu(\omega)] \right\}}, \tag{34}$$

which, upon substitution of the perturbation quantities

$$\begin{aligned} a_c &= 1 - \frac{c_0^2}{c^2}, \\ a_\nu &= i\nu(\omega) + \mathcal{H}[\nu(\omega)], \end{aligned} \tag{35}$$

expands as

$$R(\omega) = \left[\frac{1}{4} a_c - \frac{c_0}{2\omega} a_\nu(\omega) \right] + \left[\frac{1}{8} a_c^2 - \frac{1}{4} \frac{c_0}{\omega} a_c a_\nu(\omega) + \frac{1}{4} \frac{c_0^2}{\omega^2} a_\nu^2(\omega) \right] + \ldots \ . \tag{36}$$

From an inverse point of view, the key difference between this general attenuation case and the nearly-constant Q case (equation 2), is that the former has many more associated unknowns (i.e., one coefficient for each frequency in a given experiment) than the latter (i.e., one Q value).

Let us proceed as before, by forming inverse series $a_\nu = a_{\nu_1} + a_{\nu_2} + \ldots$ and $a_c = a_{c_1} + a_{c_2} + \ldots$, and substituting these into equation (36). When we attempt to separate out at first order the variability in R due to a_ν, that is, by solving

$$R(\omega) = \frac{1}{4} a_{c_1} - \frac{c_0}{2\omega} a_{\nu_1}(\omega), \tag{37}$$

for a_{α_1}, the ill-posedness of the problem becomes apparent: a new unknown is produced at every frequency. To solve the problem we must bring further information to it. In fact, the nearly-constant Q case we have used in earlier sections is an example of doing just that, by supplying a more complete initial specification of the model type. This renders the problem well-posed. Prior information in the form of parameter values may also permit a solution, a fact that is roughly in keeping with the conclusions of several studies on the more general absorptive inverse scattering problem (Carrion and VerWest, 1987; Innanen and Weglein, 2007). For instance, suppose further that at a certain reference frequency ω_0, for which $R(\omega_0) \equiv R_{\text{ref}}$ is measured, we know the attenuation coefficient: $a_{\text{ref}} \equiv a_{\nu_1}(\omega_0)$. In this circumstance $a_\nu \approx a_{\nu_1}(\omega)$ in equation (38) may be solved for at any arbitrary frequency with

$$a_\nu(\omega) \approx \frac{2\omega}{c_0} \left[R_{\text{ref}} - R(\omega) \right] + \left(\frac{\omega}{\omega_0} \right) a_{\text{ref}}. \tag{38}$$

In summary, for the case of a general attenuation coefficient, with some prior information the problem remains technically tractable, which broadens the range of model types that may be determined using absorptive reflectivity. However, some attractive features of the two parameter law (or any absorption law with a specified frequency dependence), for instance its overdetermined nature, are lost.

Absorptive incidence medium

The incidence medium has thus far been modelled as non-attenuating. If the overburden is also attenuative, the reflection coefficient is a function of this altered type of contrast across the boundary, to wit, from an incidence Q_0 to a target Q. Let us briefly demonstrate that the basic activity of the algorithm nevertheless remains intact if the overburden is absorptive, with only one of its ingredients, and the interpretation of the computed a_Q perturbation, in the final step when a target Q is being determined, needing change. If absorption is included in the incidence medium through Q_0, and the reference frequency ω_r is constant, the reflection coefficient at normal incidence becomes

$$R(\omega) = \frac{1 - \frac{c_0}{c}\left[1 + \frac{F(\omega)}{Q}\right]\left[1 + \frac{F(\omega)}{Q_0}\right]^{-1}}{1 + \frac{c_0}{c}\left[1 + \frac{F(\omega)}{Q}\right]\left[1 + \frac{F(\omega)}{Q_0}\right]^{-1}}. \tag{39}$$

Defining

$$\begin{aligned} a_c &= 1 - \frac{c_0^2}{c^2}, \\ a_Q &= 1 - \frac{Q_0}{Q}, \end{aligned} \tag{40}$$

and proceeding as before, $R(\omega)$ expands about small a_c and a_Q as

$$R(\omega) = \left[\frac{1}{4}a_c - \frac{1}{2}\frac{F(\omega)}{Q_0}\left(1 - \frac{F(\omega)}{Q_0}\right)a_Q\right] + \left[\frac{1}{8}a_c^2 + \frac{1}{4}\frac{F^2(\omega)}{Q_0^2}\left(1 - \frac{F(\omega)}{Q_0}\right)^2 a_Q^2\right] + \ldots \ . \tag{41}$$

If we define a new function F_{Q_R}, where

$$F_{Q_R}(\omega) \equiv \frac{F(\omega)}{Q_0}\left(1 - \frac{F(\omega)}{Q_0}\right), \tag{42}$$

containing only experimental variables and parameters from the medium of incidence, assumed known, we recover a mathematical framework indistinguishable from the AVF inversion in the acoustic reference case. Specifically, by making this replacement in equation (41) and comparing the result to equation (19), we surmise that the form of the inversion equations (20)–(22) is in essence maintained, and, therefore, that AVF/AVA inversion with non-attenuating incidence media contains most of what we need to know about the inverse problem for both types of incidence media.

Notice, however, that because of the definition of a_Q in equation (40), the limit $Q_0 \rightarrow \infty$, which we might expect to reduce the equations to the previous (non-attenuating incidence medium) case, is not permissible. The consequence of taking this illegitimate limit to modeling and/or inversion with equation (41) is that the reflection coefficient will be misinterpreted as being due to P-wave velocity contrasts alone. It is important to correctly characterize the incidence medium at the outset of the analysis. It should also be emphasized that to estimate an R such as that in equation (39) from seismic data would require

that the attenuation due to the overburden first be compensated for. In the discussion section we include some additional comments on the reasons why we have chosen to focus on a non-attenuating overburden.

Anelastic target medium

An extension of the current methods to the full multicomponent anelastic problem is beyond the scope of this paper, but within a simplified anelastic environment we may get a preliminary sense of that result. We begin with the Zoeppritz equations, and consider solutions generated using Cramer's rule (e.g., Keys, 1989). If we consider a plane P-wave (in an elastic medium with P-wave velocity α_0, S-wave velocity β_0, and density ρ_0) obliquely incident upon an anelastic boundary, the Zoeppritz equations, modified to incorporate a compressional quality factor Q_P and a shear quality factor Q_S in addition to target α, β, ρ values, can be expressed in a simple matrix form and, ultimately, solved for P and S reflection coefficients. We have:

$$\mathcal{A}\begin{bmatrix} R_P \\ R_S \\ T_P \\ T_S \end{bmatrix} = \mathbf{b}, \tag{43}$$

where

$$\mathbf{b} = \begin{bmatrix} X \\ (1-X^2)^{1/2} \\ 2BX(1-X^2)^{1/2} \\ 1-2B^2X^2 \end{bmatrix}, \tag{44}$$

$$\mathcal{A} = \begin{bmatrix} -X & -(1-B^2X^2)^{1/2} & CX & -(1-D^2X^2)^{1/2} \\ (1-X^2)^{1/2} & -BX & (1-C^2X^2)^{1/2} & DX \\ 2B^2X(1-X^2)^{1/2} & B(1-2B^2X^2) & 2AD^2X(1-C^2X^2)^{1/2} & -AD(1-2D^2X^2) \\ -(1-2B^2X^2) & 2B^2X(1-B^2X^2)^{1/2} & AC(1-2D^2X^2) & 2AD^2X(1-D^2X^2)^{1/2} \end{bmatrix}, \tag{45}$$

$X = \sin\theta$, and where the constants A through D, nominally containing elastic parameter ratios, are modified as follows:

$$A = \frac{\rho}{\rho_0}, \quad B = \frac{\beta_0}{\alpha_0}, \quad C = \frac{\alpha}{\alpha_0}\left[1+\frac{F_P}{Q_P}\right]^{-1}, \quad D = B\frac{\beta}{\beta_0}\left[1+\frac{F_S}{Q_S}\right]^{-1}, \tag{46}$$

where

$$F_P(\omega) = \frac{i}{2} - \frac{1}{\pi}\log\left(\frac{\omega}{\omega_{r_P}}\right), \quad F_S(\omega) = \frac{i}{2} - \frac{1}{\pi}\log\left(\frac{\omega}{\omega_{r_S}}\right), \tag{47}$$

and where the quantities ω_{r_P} and ω_{r_S} are, respectively, P- and S-wave reference frequencies. We will assume these reference frequencies are known a priori when we come to consider the inverse problem.

Next, we expand the elements of $\mathcal{A}$ in equation (43) about $X = 0$ (since both P and S reflections are being considered, we expand about $\sin\theta$, not $\sin^2\theta$, as before). For instance, $\mathcal{A}$ accurate to second order in $\sin\theta$ has the form:

$$\mathcal{A} \approx \begin{bmatrix} -X & -(1-\frac{1}{2}B^2X^2) & CX & -(1-\frac{1}{2}D^2X^2) \\ 1-\frac{1}{2}X^2 & -BX & 1-\frac{1}{2}C^2X^2 & DX \\ 2B^2X\left(1-\frac{1}{2}X^2\right) & B(1-2B^2X^2) & 2AD^2X\left(1-\frac{1}{2}C^2X^2\right) & -AD(1-2D^2X^2) \\ -(1-2B^2X^2) & 2B^2X\left(1-\frac{1}{2}B^2X^2\right) & AC(1-2D^2X^2) & 2AD^2X\left(1-\frac{1}{2}D^2X^2\right) \end{bmatrix}. \tag{48}$$

With the final aim of solving for R_P and R_S in mind, we also form the auxiliary matrix $\mathcal{A}_P$ by replacing the first column of $\mathcal{A}$ with $\mathbf{b}$, and the auxiliary matrix $\mathcal{A}_S$ by replacing the second column of $\mathcal{A}$ with $\mathbf{b}$. Next, we express the factors A, C, and D in terms of perturbations measuring the relative change in the five parameters across the boundary, which we give the form:

$$a_\alpha = 1-\alpha_0^2/\alpha^2,\ a_\beta = 1-\beta_0^2/\beta^2,\ a_\rho = 1-\rho_0/\rho,\ a_{Q_P} = 1/Q_P,\ a_{Q_S} = 1/Q_S, \tag{49}$$

and substitute them into equations (46), to obtain:

$$\begin{aligned} A &= 1 + a_\rho + a_\rho^2 + ... \\ C &= 1 + \frac{1}{2}a_\alpha - F_P a_{Q_P} + \frac{3}{8}a_\alpha^2 - \frac{F_P}{2}a_\alpha a_{Q_P} + F_P^2 a_{Q_P}^2 + ... \\ D &= B\left(1 + \frac{1}{2}a_\beta - F_S a_{Q_S} + \frac{3}{8}a_\beta^2 - \frac{F_S}{2}a_\beta a_{Q_S} + F_S^2 a_{Q_S}^2 + ...\right). \end{aligned} \tag{50}$$

When the above quantities are further substituted into $\mathcal{A}$, $\mathcal{A}_P$, and $\mathcal{A}_S$, their determinants may be organized in increasing order in the five perturbations:

$$\begin{aligned} \det\mathcal{A} &= \det\mathcal{A}^{(0)} + \det\mathcal{A}^{(1)} + \det\mathcal{A}^{(2)} + ..., \\ \det\mathcal{A}_P &= \det\mathcal{A}_P^{(1)} + \det\mathcal{A}_P^{(2)} + ..., \\ \det\mathcal{A}_S &= \det\mathcal{A}_S^{(1)} + \det\mathcal{A}_S^{(2)} + ..., \end{aligned} \tag{51}$$

where superscript (i) indicates i'th order in any combination of the perturbations in equation (49). We next use Cramer's rule to generate series expressions for R_P and R_S, also in increasing powers of the perturbations:

$$R_P = \frac{\hat{\det}\mathcal{A}_P}{\hat{\det}\mathcal{A}} = \hat{\det}\mathcal{A}_P^{(1)} + \left(\hat{\det}\mathcal{A}_P^{(2)} - \hat{\det}\mathcal{A}_P^{(1)}\hat{\det}\mathcal{A}^{(1)}\right) + ..., \tag{52}$$

and likewise

$$R_S = \hat{\det}\mathcal{A}_S^{(1)} + \left(\hat{\det}\mathcal{A}_S^{(2)} - \hat{\det}\mathcal{A}_S^{(1)}\hat{\det}\mathcal{A}^{(1)}\right) + ..., \tag{53}$$

where for any $\mathcal{Y}$, $\hat{\det}\mathcal{Y} \equiv \det\mathcal{Y}/\det\mathcal{A}^{(0)}$. Equations (52) and (53) are the anelastic extensions of equation (14), representing series formulas for the approximation of the two reflection coefficients associated with a plane elastic P-wave incident upon an anelastic

boundary. To evaluate the formulas we compute the necessary determinants and organize the results in orders of a_α, a_β, a_ρ, a_{Q_p} and a_{Q_s}. An approximation accurate to n'th order in these perturbations requires three truncations at n'th order: once in equations (50), again in (51), and finally in (52)/(53) for R_P/R_S. Explicitly, and accurate to second order in $\sin\theta$, i.e., beginning with the approximation of $\mathcal{A}$ in equation (48), we have

$$R_P(\omega,\theta) = R_{P_1} + R_{P_2} + ..., \tag{54}$$

where

$$R_{P_1}(\omega,\theta) = \Gamma^P_\alpha a_\alpha + \Gamma^P_\beta a_\beta + \Gamma^P_\rho a_\rho + \Gamma^P_{Q_P} a_{Q_P} + \Gamma^P_{Q_S} a_{Q_S}, \tag{55}$$

$$\begin{aligned} R_{P_2}(\omega,\theta) =& \Gamma^P_{\alpha\alpha}\ a^2_\alpha + \Gamma^P_{\beta\beta}\ a^2_\beta + \Gamma^P_{\rho\rho}\ a^2_\rho + \Gamma^P_{Q_PQ_P}\ a^2_{Q_P} + \Gamma^P_{Q_SQ_S}\ a^2_{Q_S} \\ &+ \Gamma^P_{\alpha\beta}\ a_\alpha a_\beta + \Gamma^P_{\alpha\rho}\ a_\alpha a_\rho + \Gamma^P_{\alpha Q_P}\ a_\alpha a_{Q_P} + \Gamma^P_{\alpha Q_S}\ a_\alpha a_{Q_S} \\ &+ \Gamma^P_{\beta\rho}\ a_\beta a_\rho + \Gamma^P_{\beta Q_P}\ a_\beta a_{Q_P} + \Gamma^P_{\beta Q_S}\ a_\beta a_{Q_S} + \Gamma^P_{\rho Q_P}\ a_\rho a_{Q_P} \\ &+ \Gamma^P_{\rho Q_S}\ a_\rho a_{Q_S} + \Gamma^P_{Q_PQ_S}\ a_{Q_P} a_{Q_S}, \end{aligned} \tag{56}$$

etc., and

$$R_S(\omega,\theta) = R_{S_1} + R_{S_2} + ..., \tag{57}$$

where

$$R_{S_1}(\omega,\theta) = \Gamma^S_\alpha a_\alpha + \Gamma^S_\beta a_\beta + \Gamma^S_\rho a_\rho + \Gamma^S_{Q_P} a_{Q_P} + \Gamma^S_{Q_S} a_{Q_S}, \tag{58}$$

$$\begin{aligned} R_{S_2}(\omega,\theta) =& \Gamma^S_{\alpha\alpha}\ a^2_\alpha + \Gamma^S_{\beta\beta}\ a^2_\beta + \Gamma^S_{\rho\rho}\ a^2_\rho + \Gamma^S_{Q_PQ_P}\ a^2_{Q_P} + \Gamma^S_{Q_SQ_S}\ a^2_{Q_S} \\ &+ \Gamma^S_{\alpha\beta}\ a_\alpha a_\beta + \Gamma^S_{\alpha\rho}\ a_\alpha a_\rho + \Gamma^S_{\alpha Q_P}\ a_\alpha a_{Q_P} + \Gamma^S_{\alpha Q_S}\ a_\alpha a_{Q_S} \\ &+ \Gamma^S_{\beta\rho}\ a_\beta a_\rho + \Gamma^S_{\beta Q_P}\ a_\beta a_{Q_P} + \Gamma^S_{\beta Q_S}\ a_\beta a_{Q_S} + \Gamma^S_{\rho Q_P}\ a_\rho a_{Q_P} \\ &+ \Gamma^S_{\rho Q_S}\ a_\rho a_{Q_S} + \Gamma^S_{Q_PQ_S}\ a_{Q_P} a_{Q_S}, \end{aligned} \tag{59}$$

etc. The coefficients Γ, which are generally functions of θ, ω and incidence medium parameters, within the current approximation are provided in Appendix A.

In Figure 6, the coefficients R_P and R_S are plotted as functions of θ and $f = \omega/2\pi$ for parameters $\rho_0 = 2.1$g/cm^3, $\rho = 2.1$g/cm^3, $\alpha_0 = 3000$m/s, $\alpha = 3500$m/s, $\beta_0 = 1500$m/s, $\beta = 1700$m/s, $Q_P = 5$, and $Q_S = 5$. Exact coefficients are in the left column, linear approximations (i.e., $R_P \approx R_{P_1}$ and $R_S \approx R_{S_1}$) are in the center, and nonlinear approximations accurate to second order in the perturbations (i.e., $R_P \approx R_{P_1} + R_{P_2}$ and $R_S \approx R_{S_1} + R_{S_2}$) are in the right column. In all cases, regimes of (small) angle are noted where the approximations are accurate. In Figure 7, for instance, extractions of the same R_P and R_S are plotted vs. angle (left column) for fixed $f = 40$Hz, and vs. frequency (right column) for fixed $\theta_0 = 11^\circ$.

Let us treat the inverse problem in the linear approximation, i.e., assuming $R_P \approx R_{P_1}$ and $R_S \approx R_{S_1}$, in which case we have

$$\begin{aligned} R_P(\omega,\theta_0) &= \Gamma^P_\alpha(\theta_0) a_\alpha + \Gamma^P_\beta(\theta_0) a_\beta + \Gamma^P_\rho(\theta_0) a_\rho + \Gamma^P_{Q_P}(\omega,\theta_0) a_{Q_P} + \Gamma^P_{Q_S}(\omega,\theta_0) a_{Q_S}, \\ R_S(\omega,\theta_0) &= \Gamma^S_\beta(\theta_0) a_\beta + \Gamma^S_\rho(\theta_0) a_\rho + \Gamma^S_{Q_S}(\omega,\theta_0) a_{Q_S}. \end{aligned} \tag{60}$$

Taking differences of these coefficients for pairs of frequencies ω_1 and ω_2 permits the Q_P and Q_S perturbations to be solved for. The Q_S perturbation is solved for using R_S:

$$a_{Q_S} = \frac{R_S(\omega_1, \theta_0) - R_S(\omega_2, \theta_0)}{\Gamma^S_{Q_S}(\omega_1, \theta_0) - \Gamma^S_{Q_S}(\omega_2, \theta_0)}. \tag{61}$$

The Q_P perturbation may then be solved for through the difference

$$R_P(\omega_1, \theta_0) - R_P(\omega_2, \theta_0) = \left[\Gamma^P_{Q_P}(\omega_1, \theta_0) - \Gamma^P_{Q_P}(\omega_2, \theta_0)\right] a_{Q_P} + \left[\Gamma^P_{Q_S}(\omega_1, \theta_0) - \Gamma^P_{Q_S}(\omega_2, \theta_0)\right] a_{Q_S}, \tag{62}$$

from which, and using equation (61),

$$a_{Q_P} = \frac{R_P(\omega_1, \theta_0) - R_P(\omega_2, \theta_0)}{\Gamma^P_{Q_P}(\omega_1, \theta_0) - \Gamma^P_{Q_P}(\omega_2, \theta_0)} - \frac{\Gamma^P_{Q_S}(\omega_1, \theta_0) - \Gamma^P_{Q_S}(\omega_2, \theta_0)}{\Gamma^P_{Q_P}(\omega_1, \theta_0) - \Gamma^P_{Q_P}(\omega_2, \theta_0)}[R_S(\omega_1, \theta_0) - R_S(\omega_2, \theta_0)]. \tag{63}$$

It is proper to think of these linear estimates of a_{Q_P} and a_{Q_S} as being functions of ω_1, ω_2, and θ_0, since their accuracy in general depends on the specific part of the full data set (in this case, the full data set is R_P and R_S over the full frequency and angle range) being used. In Figure 8 we observe the results of applying these linearized formulas to synthetically derived, exact, reflection coefficients. Some care is required in choosing angles. For instance, our inverse formulas absent nonlinear correction rely on the $R_P \approx R_{P_1}$, $R_S \approx R_{S_1}$ approximations being accurate, hence θ should not be chosen too large. However, $R_S = 0$ at $\theta = 0$, hence if θ is chosen too small, the signal with which the shear parameter estimations are carried out will be too low (although, judging from equation (63), this may be a convenient regime in which to more straightforwardly estimate the compressive parameters). The angle used in Figure 7, $\theta = 11^\circ$, is also used here. In Figure 8, Q_P and Q_S are recovered for ranges of pairs of frequencies as before. Similar accuracies are noted in comparison to the two-parameter AVF results produced in equations (20)–(21).

This may proceed for the other parameters by varying θ, and for higher orders also, as we have illustrated in earlier sections. The core activity in the estimation of Q perturbations remains the frequency differencing of the reflection coefficients. In spite of the increased complexity in terms of parameters and physical phenomena, we again discern that the basic data interrogation procedure seen in equation (20) is preserved.

DISCUSSION

The purpose of this paper is to discuss some of the principle theoretical features of the direct inversion of a largely untapped type of seismic reflectivity information: that associated with a rapid change from a predominantly elastic overburden to a highly attenuative target. The range of available formulas suggests that, given accurate estimates of the reflection coefficient at an anelastic boundary, simultaneous variations in multiple an-acoustic or anelastic target parameters may be directly determined.

In spite of the theoretical nature of the development and results we present, we are, ultimately, interested in the application of the formulas we derive in this paper to field data.

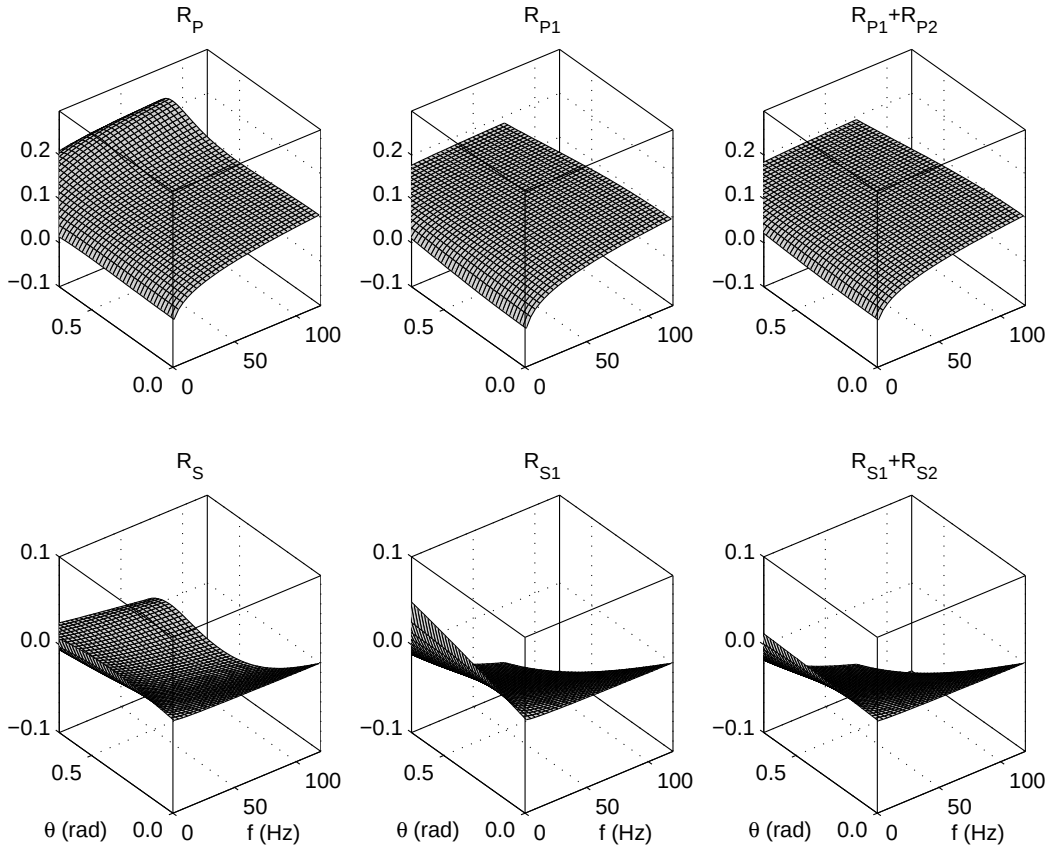

FIG. 6. The real parts of R_P and R_S plotted for a range of angles and frequencies. Left column: exact R_P and R_S, calculated using equation (43); middle column: R_P and R_S, accurate to first order in the perturbations and $\sin^2\theta$, calculated using linearly truncated versions of equations (54) and (57); right column: R_P and R_S accurate to second order in the perturbations and first order in $\sin^2\theta$, calculated using second order truncations of equations (54) and (57).

This will require one of two steps beyond what we have presented in this paper: either (1) an extension of these results to accommodate a much more complicated Earth, such that the seismic response is modelled (at least) as being due to a stack of homogeneous layers, or (2) the extraction and isolation of an individual event from a seismic data set, and an estimation of its associated (absorptive) reflection coefficient. The first of these routes is, of course, of interest and, if it is to be carried out using a perturbation approach, requires the solution of a more complete inverse scattering problem. This has been, and continues to be, studied by ourselves and others (e.g., Carrion and VerWest, 1987; Ribodetti and Virieux, 1998; Innanen and Weglein, 2007; Mulder and Hak, 2009; Innanen and Lira, 2010; Hak and Mulder, 2010).

In this paper we are concerned with the second, more specialized problem, of analyzing an isolated event which, through an interpretive step, has been identified as a primary reflecting from a likely attenuative target. Because variations of R with frequency drive the procedures, the local spectrum of an identified event will need to be estimated. This is not a straightforward task, but fortunately, a wide array of methods for determining these spectra has been developed in recent years (e.g., Margrave, 1997; Margrave et al., 2003;

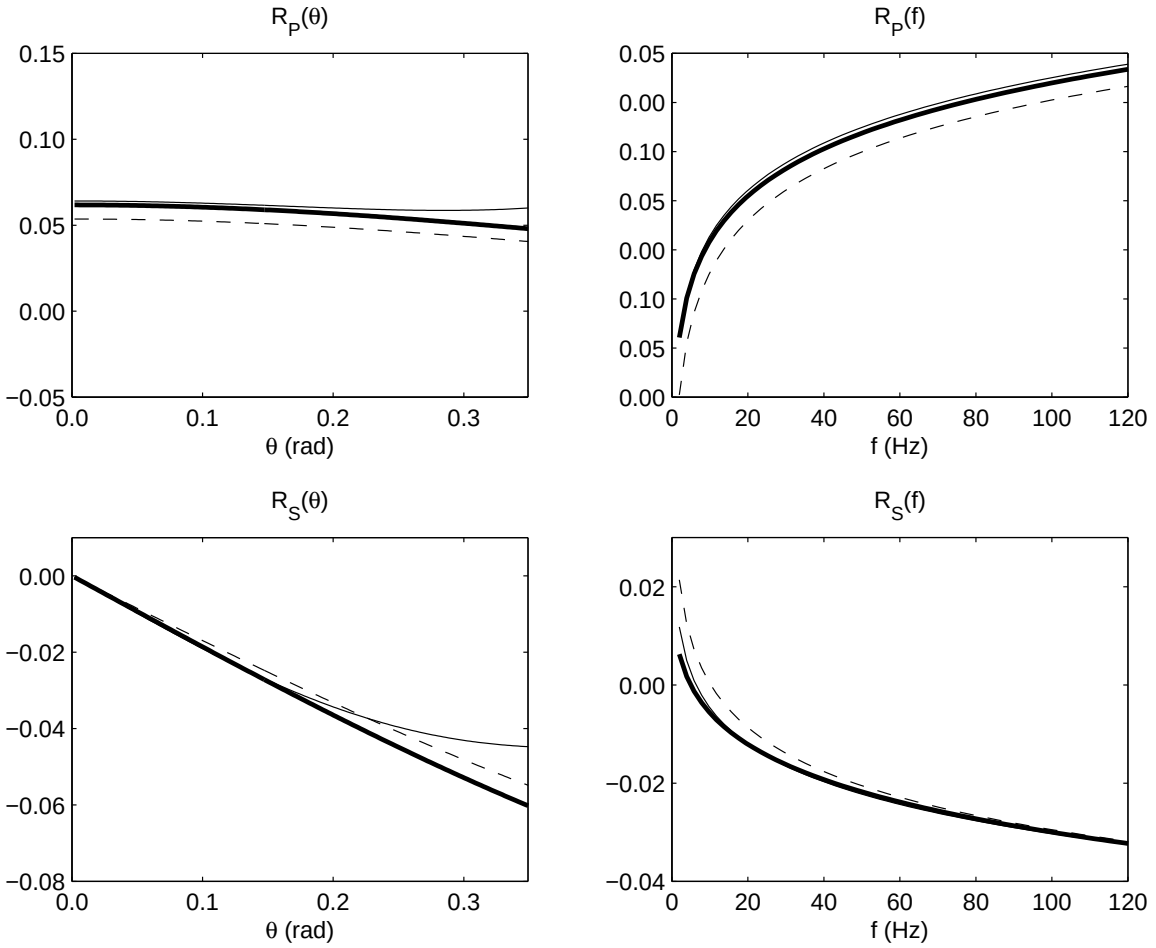

FIG. 7. Real parts of R_P and R_S values extracted from Figure 6. Left column: R_P and R_S plotted as functions of angle for fixed $f = \omega/2\pi = 40Hz$. Right column: R_P and R_S plotted as functions of frequency f for fixed $\theta = 11°$. Exact coefficients are plotted as solid lines, first order approximations as dashed lines, and second order approximations as bold solid lines.

Odebeatu et al., 2006), usually to facilitate nonstationary seismic processing. One such approach which shows promise to this end has recently been implemented in multiple dimensions and used as a tool for seismic interpolation (Naghizadeh and Innanen, 2010). It is currently being studied for its ability to extract local reflection coefficient spectra from a seismic trace and/or section, thereby acting as a front-end preprocessing tool for inversion of the type we have described here.

Absorptive AVF/AVA inverse procedures are possible only because of the dispersive component of absorptive wave propagation, in particular, for the purposes of this paper, as it manifests in reflection coefficients. The role of dispersion in direct absorptive inversion, both linear and nonlinear, in simplified environments such as these, and in more complete inverse scattering formulations, is critical. Neglecting it when beginning to pose the absorptive seismic scattering problem can lead to, amongst other things, intrinsically ambiguous inverse algorithms for reflection data (as pointed out by Mulder and Hak, 2009; Hak and Mulder, 2010).

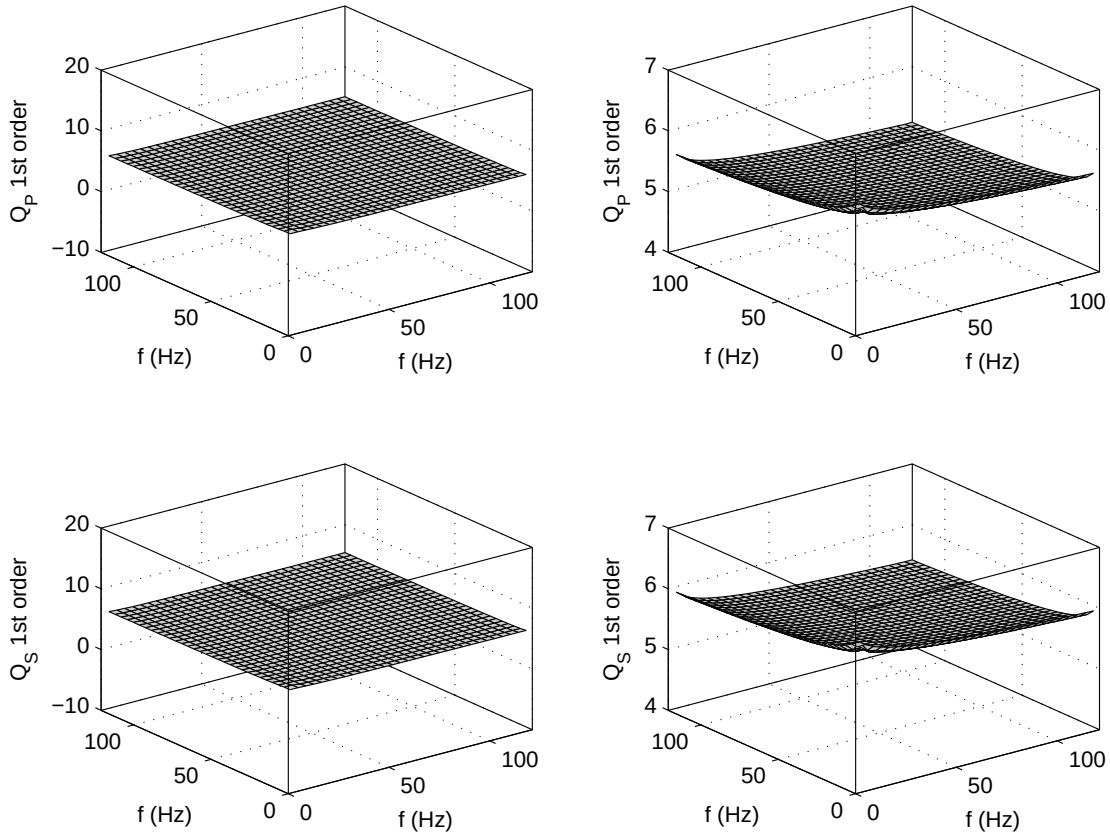

FIG. 8. Recovered Q_P and Q_S values accurate to first order (actual values $Q_P = Q_S = 5$) using exact synthetic R_P, R_S values, calculated using equation (43), as input for the AVF inverse formulas in equations (61) and (63), over a range of frequency pairs and with $\theta = 11^\circ$. Left column: recovered Q_P, Q_S values; right column: detail of same.

Procedures with AVF and AVA flavors, as well as mixtures of the two, have been examined. AVF is used in this paper to refer to any formula in which Q, Q_P, or Q_S are determined with values of R, R_P, or R_S at different frequencies. The anelastic formulas are considered to be in the AVF category, for instance, even though they were by necessity carried out at oblique incidence. Indeed, if we had gone on to use these expressions to further estimate the P-wave and S-wave velocity and density of the target, different angles would certainly have to have been used. We nevertheless consider these to be AVF formulas; the term AVA is here reserved for problems in which the dispersion of the target medium was expressed explicitly in terms of an angle variation.

Since Q dominates in prescribing the AVF variability of the reflection strength, whereas it co-determines the AVA variability alongside the much more influential P-wave velocity (and other parameters in the anelastic case), thus leading to a more sensitive separation problem, it would appear that in posing an absorptive AVA inverse problem we are unnecessarily complicating matters. The main reason we have included AVA methods in this paper is because they form a bridge between the theory in this paper and the more general theories for absorptive inverse scattering. It has, at least in the past, been convenient to

adopt angle θ and k_z as variables in linear and nonlinear inversion for Q profiles and for posing Q compensation: variation of data with θ is used to separate out the influences of multiple parameters, and k_z, the Fourier dual of depth, is varied to construct the spectrum of the profile and/or the operator for inverse Q filtering (Innanen and Lira, 2010). Our auxiliary interest in the separability of absorptive parameters with a specified k_z, coupled with a wish to survey as many different approaches to the problem as possible, has led us to pose the inversion both ways.

CONCLUSIONS

We have carried out a theoretical examination of a potentially valuable inverse procedure, i.e., the direct estimation of absorptive medium properties from absorptive reflectivity information. We are buoyed by the wave-theoretic prediction that low-Q targets do indeed imprint themselves in their corresponding reflection coefficients, and further by the earlier-referenced field studies and discussions suggesting that these imprints appear at detectable levels in our data. The result is a framework, analogous to AVO/AVA based estimation of acoustic or elastic target medium properties, in which the output are target Q (or Q_P and Q_S) values, as well as P- and S-wave velocities, density, etc.

All linear and nonlinear absorptive AVF/AVA problems we have studied have proven tractable, provided the dispersion was given a functional form a priori (e.g., the $\log(\omega/\omega_r)$ term in the nearly-constant Q model). If the frequency dependence of the attenuation parameter is left as a freely-varying unknown, prior information in other forms must be utilized.

The AVF/AVA modes we have examined are: varying $R(\omega, \theta)$ with ω both at fixed $\theta = 0$ and $\theta \neq 0$, varying $R(k_z, \theta)$ with θ at fixed k_z, and varying $R_P(\omega, \theta)$, $R_S(\omega, \theta)$ with ω for fixed $\theta \neq 0$. The relative numerical stability of the results suggests that using the AVF signature of R explicitly, i.e., varying ω, is more robust than the AVA parametrization.

Nonlinear corrections would appear to be a key element of the inversion in the presence of low-Q targets. For instance, if the target Q value is in the range 5-10, the linearized estimate, depending on which data type and formula are used, could be in error by anywhere from 10-50%. In addition to reducing the bulk error, the second order correction "flattens" the estimate when it is plotted over all pairs of frequency or angle, meaning, the variation in accuracy of the results is lowered considerably. Nevertheless, the linearized estimates may often be more than sufficient to detect and roughly characterize a fluid target.

As with the more general problem of absorptive inverse scattering, the final aim is to cast the problem in a suitably complete anelastic environment, possibly coupled with anisotropy. This step, and the problem of extracting with sufficiently high fidelity the spectrum of an identified reflection, remain what we consider the primary issues requiring further analysis. Here we have lain some of the groundwork for development towards this end. In doing so we have demonstrated that certain properties of absorptive AVF/AVA inversion are apparently independent of the complexity of the model type. In particular, differencing of reflection strengths across frequency (or its proxy in the angle domain) evidently drives the procedure, whether in a two-parameter acoustic/absorptive physical

setting or a five-parameter anelastic setting, and also regardless of whether the incidence medium is attenuating or non-attenuating. We expect such generalities to remain as more complete versions of these methods are developed.

ACKNOWLEDGMENTS

The author is grateful to the sponsors and personnel of CREWES, as well as Bill Harlan and an anonymous reviewer for their feedback and suggestions. Financial support was provided by CREWES and NSERC.

APPENDIX A: COEFFICIENTS OF EXPANSION OF ANELASTIC R_P AND R_S

The coefficients in the expansions in equation (56) are

$$\Gamma^P_\alpha = \frac{1}{4}(1+\sin^2\theta),\quad \Gamma^P_\beta = -2B^2\sin^2\theta,\quad \Gamma^P_\rho = \frac{1}{2}(1-4B^2\sin^2\theta),\quad \Gamma^P_{Q_P} = -\frac{1}{2}F_P(1+\sin^2\theta),$$

$$\Gamma^P_{Q_S} = 4F_SB^2\sin^2\theta,\quad \Gamma^P_{\alpha\alpha} = \frac{1}{8}+\frac{1}{4}\sin^2\theta,\quad \Gamma^P_{\beta\beta} = B^2(B-2)\sin^2\theta,\quad \Gamma^P_{\rho\rho} = \frac{1}{4}-B\left(\frac{1}{4}-B^2+B\right)\sin^2\theta,$$

$$\Gamma^P_{Q_PQ_P} = F_P^2\left(\frac{1}{4}+\frac{3}{4}\sin^2\theta\right),\quad \Gamma^P_{Q_SQ_S} = 2F_S^2B^2(2B-3)\sin^2\theta,\quad \Gamma^P_{\alpha\beta} = 0,\quad \Gamma^P_{\alpha\rho} = 0,$$

$$\Gamma^P_{\alpha Q_P} = -\frac{1}{2}F_P\sin^2\theta,\quad \Gamma^P_{\alpha Q_S} = 0,\quad \Gamma^P_{\beta\rho} = B^2(2B-1)\sin^2\theta,\quad \Gamma^P_{\beta Q_P} = 0,$$

$$\Gamma^P_{\beta Q_S} = 4B^2F_S(1-B)\sin^2\theta,\quad \Gamma^P_{\rho Q_P} = 0,\quad \Gamma^P_{\rho Q_S} = 2B^2F_S(1-2B)\sin^2\theta,\quad \Gamma^P_{Q_PQ_S} = 0,$$

and the coefficients in equation (59) are

$$\Gamma^S_\alpha = 0,\quad \Gamma^S_\beta = -B\sin\theta,\quad \Gamma^S_\rho = -\left(B+\frac{1}{2}\right)\sin\theta,\quad \Gamma^S_{Q_P} = 0,$$

$$\Gamma^S_{Q_S} = 2BF_S\sin\theta,\quad \Gamma^S_{\alpha\alpha} = 0,\quad \Gamma^S_{\beta\beta} = -\frac{3}{4}B\sin\theta,\quad \Gamma^S_{\rho\rho} = -\frac{1}{2}\sin\theta,$$

$$\Gamma^S_{Q_PQ_P} = 0,\quad \Gamma^S_{Q_SQ_S} = -2BF_S^2\sin\theta,\quad \Gamma^S_{\alpha\beta} = \frac{1}{4}B\sin\theta,\quad \Gamma^S_{\alpha\rho} = \frac{1}{4}\left(B-\frac{1}{2}\right)\sin\theta,$$

$$\Gamma^S_{\alpha Q_P} = 0,\quad \Gamma^S_{\alpha Q_S} = -\frac{1}{2}BF_S\sin\theta,\quad \Gamma^S_{\beta\rho} = \frac{1}{4}\left(B-\frac{1}{2}\right)\sin\theta,\quad \Gamma^S_{\beta Q_P} = -\frac{1}{2}BF_P\sin\theta,$$

$$\Gamma^S_{\beta Q_S} = BF_S\sin\theta,\quad \Gamma^S_{\rho Q_P} = \frac{1}{4}F_P\left(1-2B\right)\sin\theta,\quad \Gamma^S_{\rho Q_S} = \frac{1}{4}F_S(1-2B)\sin\theta,\quad \Gamma^S_{Q_PQ_S} = 0.$$

REFERENCES

Aki, K. and P. G. Richards, 2002, Quantitative seismology: University Science Books, 2nd edition.

Borcherdt, R. D., 1977, Reflection and refraction of type-II S waves in attenuating media: Bull. Seism. Soc. Am., **67**, 43–67.

———, 2009, Viscoelastic waves in layered media: Cambridge University Press.

Carrion, P. M. and B. VerWest, 1987, A procedure for inverting seismic data to obtain Q-profiles: Inverse Problems, 65–71.

Castagna, J. P., S. Sun, and R. W. Siegfried, 2003, Instantaneous spectral analysis: detection of low-frequency shadows associated with hydrocarbons: The Leading Edge, 120–127.

Chapman, M., E. Liu, and X. Y. Li, 2006, The influence of fluid-sensitive dispersion and attenuation on AVO analysis: Geophysical Journal International, **167**, 89–105.

de Hoop, A. T., C. H. Lam, and B. J. Kooij, 2005, Parametrization of acoustic boundary absorption and dispersion properties in time domain source/receiver reflection measurement: J. Acoust. Soc. Am., **118**, 654–660.

Hak, B. and W. A. Mulder, 2010, Migration for velocity and attenuation perturbations: Geophysical Prospecting, **58**, 1–13.

Innanen, K. A., 2010a, AVF inversion of reflections from an anelastic target, *in* Proceedings of the SEG, Denver, CO, USA, Soc. Expl. Geophys.

———, 2010b, Some formulas for AVF-AVA inversion of reflections from absorptive targets, *in* Proceedings of the EAGE, Barcelona, Spain, Eur. Ass. Geosci. Eng.

Innanen, K. A. and J. E. Lira, 2010, Direct nonlinear Q compensation of seismic primaries reflecting from a stratified, two-parameter absorptive medium: Geophysics, **75**, V13–V23.

Innanen, K. A. and A. B. Weglein, 2007, On the construction of an absorptive-dispersive medium model via direct linear inversion of reflected seismic primaries: Inverse Problems, **23**, 2289–2310.

Keys, R. G., 1989, Polarity reversals in reflections from layered media: Geophysics, **54**, 900–905.

Kjartansson, E., 1979, Attenuation of seismic waves in rocks and applications in energy exploration: PhD thesis, Stanford University.

Krebes, E. S., 1984, On the reflection and transmission of viscoelastic waves–some numerical results: Geophysics, **49**, 1374–1380.

Lam, C. H., B. J. Kooij, and A. T. de Hoop, 2004, Impulsive sound reflection from an absorptive and dispersive planar boundary: J. Acoust. Soc. Am., **116**, 677–685.

Lines, L. R., F. Vasheghani, and S. Treitel, 2008, Reflections on Q: CSEG Recorder, **Dec**, 36–38.

Margrave, G. F., 1997, Theory of nonstationary linear filtering in the fourier domain with application to time-variant filtering: Geophysics, **63**, 244.

Margrave, G. F., D. Henley, M. P. Lamoureux, V. Iliescu, and J. Grossman, 2003, Gabor deconvolution revisited, *in* Proc. 76th Ann. Mtg., Dallas TX, Soc. Expl. Geophys.

Mulder, W. A. and B. Hak, 2009, An ambiguity in attenuation scattering imaging: Geophys. J. Int., **178**, 1614–1624.

Naghizadeh, M. and K. A. Innanen, 2010, Seismic data interpolation using a fast nonredundant s-transform: *submitted to* Geophysics.

Odebeatu, E., J. Zhang, M. Chapman, E. Liu, and X. Y. Li, 2006, Application of spectral decomposition to detection of dispersion anomalies associated with gas saturation: The Leading Edge, **2**, 206–210.

Quintal, B., S. M. Schmalholz, and Y. Y. Podladchikov, 2009, Low-frequency reflections from a thin layer with high attenuation caused by interlayer flow: Geophysics, **74**, N15–N23.

Ren, H., G. Goloshubin, and F. J. Hilterman, 2009, Poroelastic analysis of amplitude-

versus-frequency variations: Geophysics, **74**, N49–N54.
Ribodetti, A. and J. Virieux, 1998, Asymptotic theory for imaging the attenuation factor Q: Geophysics, **63**, 1767–1778.
Samec, P. and J. P. Blangy, 1992, Viscoelastic attenuation, anisotropy, and AVO: Geophysics, **57**, 441.
White, J. E., 1965, Reflections from lossy media: Journal of the Acoustical Society of America, **38**, 604–607.
Zhang, H. and A. B. Weglein, 2009a, Direct nonlinear inversion of multiparameter 1D acoustic media using inverse scattering subseries: Geophysics, **74**, WCD29–WCD39.
———, 2009b, Direct nonlinear inversion of multiparameter 1D elastic media using the inverse scattering series: Geophysics, **74**, WCD15–WCD27.